

Response of Cadmium Zinc Telluride Compound Semi-Conductor Detector against Gamma Photons by Efficiency Calculation: A Microdosimetry Simulation Study

Golnaz Barzgarnezhad¹, Ahmad Esmaili Torshabi^{2*}

1. Faculty of Sciences and Modern Technologies, Graduate University of Advanced Technology, Kerman, Iran
2. Faculty of Sciences and Modern Technologies, Graduate University of Advanced Technology, Kerman, Iran

ARTICLE INFO

Article type:
Original Paper

Article history:
Received: Sep 14, 2019
Accepted: Dec 12, 2019

Keywords:
Semiconductors
Radiation Dosimetry
Photons
Efficiency
Monte Carlo code

ABSTRACT

Introduction: Cadmium zinc telluride has recently been used as a compound semiconductor detector in a wide range of fields. The current study is a comprehensive investigation of the performance of this detector against the photon beam. Moreover, a comparative study was carried out with other common detectors using the Monte Carlo code by the implementation of the same strategy.

Material and Methods: During the simulation by FLUKA code, a number of photons were regarded as primary particles. It is attractive to trace each incident photon uniquely considering all possible collisions and produced secondary particles at the microdosimetry scale. In the current study, the coordinate of three-dimensional collisions location was realized at detector sensitive volume. Moreover, energy deposition was considered at each unique collision and through all interactions, totally. In addition, the physical concepts of photon interaction with detector volume were assessed, numerically. Furthermore, the effect of gold foils implemented as electrode at both sides of the detector was taken into account.

Results: The obtained results indicated the context of photoelectric and Compton scattering in photon interactions with CZT, including the number of interactions, the deposited energy, and three-dimensional collision coordinate, while the latter case is proposed as a new achievement.

Conclusion: As evidenced by the obtained results, the performance of this detector can be improved by changing material fraction and detector dimension to achieve optimum efficiency. In addition, the comparative results demonstrated that the efficiency of CZT covered by gold electrodes is superior to other common available semi-conductor detectors.

► Please cite this article as:

Barzgarnezhad G, Esmaili Torshabi A. Response of Cadmium Zinc Telluride Compound Semi-Conductor Detector against Gamma Photons by Efficiency Calculation: A Microdosimetry Simulation Study. Iran J Med Phys 2020; 17: 359-365. 10.22038/ijmp.2019.43393.1656

Introduction

In recent years, semiconductor materials, such as Cadmium Telluride (CdTe) and Cadmium Zinc Telluride (CZT), have been widely used for the construction of semi-conductor detectors as the most promising detector which is implemented at a wide range of fields [1-3]. Its high resistivity, low current leakage, and good charge transport properties have made it a robust detector [4-5]. Nonetheless, its energy resolution is significantly limited by trapping of charge carriers (i.e., electrons and holes) during their transit to the electrodes [3, 6-7].

In order to achieve high-sensitivity and efficiency, detector material and structure should be optimal to enhance maximal incident photons inside the sensitive volume of a detector. In order to realize signal generation in semiconductor detectors, the physical concept of photon interaction with the detector body must be thoroughly taken into account. This challenging issue has been extensively addressed in the literature [8-12]. Nevertheless, a major need

still exists to numerically investigate the behavior of incident photons with a typical detector in the microdosimetry scale by tracking each photon inside the sensitive volume of a detector. This numerical assessment provides valuable information, including: 1) the type of interaction, 2) the number of hits or interactions which happened inside detector body, 3) three-dimensional coordinates of location where a photon hits or interacts inside detector volume, and 4) the amount of energy released at each interaction on a case-by-case basis for each photon. The present study investigated all possible interactions which happened for typical primary gamma rays inside the crystal sensitive volume of compound semi-conductor detector. To shed more light on this issue, the detector efficiency parameter was used as a mathematical tool to calculate the ratio of incident photons to total primary photons emitted from an isotropic photon source [13-17]. By colliding each gamma within the sensitive volume of detector, its tracking starts while

photon enters into semiconductor detector body with a specific pre-defined energy till ending point. Thereafter, photon either leaves the detector with a fraction of its initial energy or disappears and gives its whole energy to ejected electrons inside detector volume. Throughout this photon trip, all possible collisions, as well as its energy deposition, will be quantitatively considered [3].

In the current study, various standard sources were simulated against CZT as a compound semiconductor detector at a microdosimetry scale to measure detector efficiency using the FLUKA Monte Carlo code(version 2011) [18-22].

FLUKA code is a multi-purpose verified simulation code which calculates the interaction and propagation of various common available particles and photons at different matters with high accuracy. The valuable results of this code have made it highly applicable in a wide range of fields, such as medical physics, dosimetry, and shielding [18-20, 23-24]. It is worthy to note that the pre-defined simulation parameters are in agreement with real experimental conditions.

After running FLUKA, the simulation results demonstrate detailed information of photons interaction with CZT materials, including energy deposition of each photon and its three-dimensional collision. Furthermore, this information can be used for the assessment of the type of each interaction as an important result for a better analysis of CZT.

This will be advantageous since the performance of CZT against photons interaction will be quantitatively understood. This microdosimetry information enables us to assess the effect of materials fraction and the dimension of the CZT detector on its efficiency. Therefore, a close correlation exists between these two parameters and photon behavior inside detector sensitive volume.

Apart from CZT, Silicon, Germanium, and Cadmium Telluride are highly applicable for monitoring ionizing radiations [25-28]. In the current study, a comparative study was performed between CZT detector regarding Si, Ge, and CdTe for a better analysis of CZT performance.

It is noteworthy that two gold foils were practically utilized as electrodes at both sides of CZT. In the present research, the effects of these foils on detector efficiency were investigated considering secondary

particles which were ejected from both foils and entered the sensitive volume of CZT.

In brief, in the current study, incident photons emitted from an isotropic gamma source were tracked on a case-by-case basis taking into account all secondary particles produced through photon trajectory inside detector sensitive volume. Secondly, numerical data on energies deposited due to the interactions of each photon were reported considering three-dimensional coordinate of each collision at the microdosimetry scale. Thirdly, for a better understanding of CZT physical properties at signal generation, the performance of CZT was compared with other common available semiconductor detectors used traditionally. Finally, the effect of electrode gold foils was quantitatively assessed to realize the share of electrodes in the production of high energy electrons due to primary photons interaction with them and the role of these electrons on final signal generation.

Materials and Methods

FLUKA (FLUKtuierende KASKade or Fluctuating Cascade developed by the Italian National Institute for Nuclear Physics (INFN) and the European Organization for Nuclear Research (CERN)) is a Monte Carlo simulation package for modelling particle transport and interactions with matter over an extended energy range for each particle [18-20, 23,24]. Complicated geometries with combinational materials are regarded as robust properties of this code that can be easily simulated, whereas experimental condition for performing the desired test is almost impossible or difficult. In the current study, CZT was simulated with $2.77 \times 2.77 \times 0.8$ cm³ dimensions. The pre-defined materials in our simulated detector were Cadmium, Zinc, and Telluride elements with 0.55, 0.05, and 0.40 fractions, respectively, the same as real CZT used experimentally. Total detector density is 6.25 g/cm³ and the atomic number of Cd, Z, and Tl are 48, and 52, respectively[5]. The irradiation source in isotropic mode is Cs-137 with 662 keV energy and with 1 cm far away from the detector, as reference. Furthermore, other energies considered in the present study included 28 keV (Iodine), 380 keV (Iridium-192), and 1250 keV (Cobalt-60) [6-7, 29].

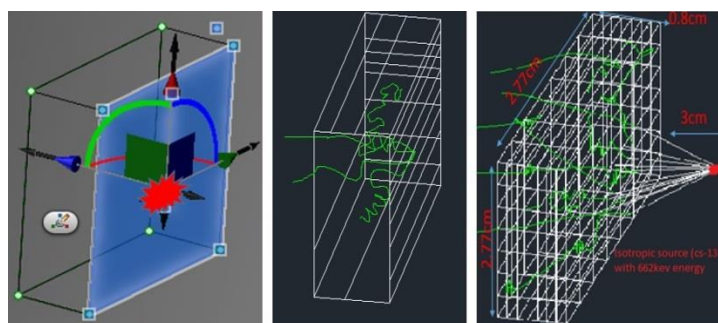


Figure 1. Schematic layout of three-dimensional semiconductor detectors in mesh structure in front of isotropic point source

Figure 1 demonstrates a schematic layout of the semi-conductor detector against a typical isotropic point source (left panel) depicting by mesh structure (right panel).

During the simulation, $277 \times 277 \times 80$ number of meshes were chosen as the optimum number inside detector volume in order to obtain the mesh size of $0.01 \times 0.01 \times 0.01$ cm³ dimension. This size is less than the range of ejected electron and it can be accurately tracked on its path length three-dimensionally inside detector sensitive volume. Mesh sizes larger than this value may increase particle-tracking error and the types of interaction will not also be recognized. Given the final results, the energy deposition of each particle inside each given mesh or cell is measured plus, apart from its three-dimensional collisions coordinate. It is worthy to note that a post-processing step is required on the FLUKA output file using a dedicated subroutine.

On a final note, CZT efficiency was compared with other common available detectors, namely Si, Ge, and CdTe [29]. It is also worth noting that the simulation parameters are the same for each detector type to have a reasonable comparison.

These parameters include detector dimension, the distance between source and detector, isotropic source characters, the number of primary photons, and the given output. Moreover, the effect of gold foil with a 0.1 mm thickness implemented as electrodes at both sides of the detector crystal volume was also investigated.

Figure 2 displays a schematic layout of gold foil which was added to the CZT detector structure (yellow foils) with the given dimensions. After irradiation, the charge carriers were gathered for generating the output pulse. To this end, the applied electric field to these electrodes should be large enough to collect charges before recombining. Thereafter, per amplifier and amplifier are utilized to produce output pulse.

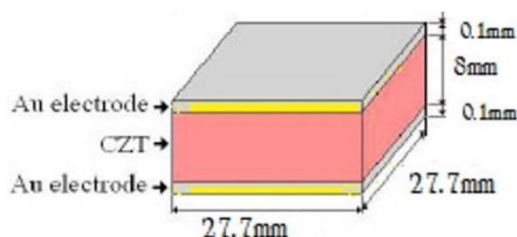


Figure 2. Schematic layout of Cadmium Zinc Telluride with gold foils in yellow color located on its both up and downsides

Final obtained results are of great help in realizing the role of electrons ejected from the foils in the performance of the detector system.

Results

Calculation results from the interaction of 662 keV photons with CZT sensitive volume are presented in Table 1. This Table consists of collision information of each incident photon as one typical event, on a case-by-case basis. As illustrated, this information includes i: the

coordinate of each collision through detector volume three-dimensionally (column 1), ii) energy deposition of scattered electrons and photons at each collision, numerically (column 2), and iii) the type of interaction as photo-electric or Compton phenomenon (column 3). In this Table, the highlighted information displays the primary photon index and total energy deposition of that photon, demonstrated at the first and second columns, respectively. In fact, among the total number of primary photons, only a fraction has interacted with detector volume and the rest have passed without any interaction. Since the given energy is less than 1.02 MeV, the pair production phenomena will not occur in this case. Therefore, two photoelectric phenomena and Compton scattering can be comprehended in this work.

On the basis of the information presented at this Table, the physical concepts of all possible photon incidents through CZT are assessed in microdosimetry scale, while total or a fraction of photon energy has been deposited as follows:

1) For primary photon with index #81, the phenomenon is photoelectric and total energy deposition is 662 keV. In this phenomenon, ejected photoelectron causes ionization at the middle part of the detector from mesh 39 to 41 on Z direction that is at 4 mm in depth along with photon beam propagation.

2) For primary photon with index #42, Compton scattering occurs, and the total energy of the ejected electron and scattered photon was spent up to 662 keV. As can be observed, the main ionization has occurred at three different sub-regions inside detector sensitive volume which started from meshes with 48, 57, and 78 indices at depth in Z direction.

3) For primary photon with index #53, the phenomenon is photoelectric; nonetheless, the ejected electron has left detector volume since a fraction of total energy has been deposited inside detector volume near downstream edge of the detector volume against beam propagation.

4) For primary photon with index #21, Compton scattering happens while a fraction of energy belonging to ejected electron has been deposited around mesh with 68 index (or 6.8 mm in detector depth) in z-direction and the scattered photon has left the detector.

Therefore, based on obtained microdosimetry results demonstrated in Table 1, photoelectric effect and Compton scattering can be easily distinguished based on deposited energy and collisions coordinate [6].

By the addition of two gold foils at both sides of CZT as electrodes, detector efficiency improved by increasing 1) the number of photons interacted with detector sensitive volume, 2) the amount of deposited energy of each interacted photons, as opposed to the same condition without gold foil. It is worth noting that the two added gold foils did not belong to detector sensitive volume during calculations process. As evidenced in this table, the number of events or photons with total deposited energy is increasing regarding CZT without electrodes.

Table 1. Selected results from the interaction of 662 keV photons in Cadmium Zinc Telluride

| Mesh detector | coordinate inside | Energy deposition at each interaction (keV) | Type of interaction |
|---------------------|-------------------|---|---------------------|
| x y z | | | |
| 139 139 39 | | 34.80 | |
| 139 139 40 | | 86.10 | |
| 141 139 40 | | 46.00 | |
| 139 138 41 | | 18.80 | |
| 140 138 41 | | 39.40 | photoelectric |
| 141 138 41 | | 12.60 | |
| 139 139 41 | | 10.90 | |
| 141 139 41 | | 200.00 | |
| Primary photon #81 | | Total E. Dept: 662.00 | |
| 139 139 68 | | 7.23 | |
| 139 139 69 | | 67.80 | |
| 140 139 69 | | 10.70 | Compton |
| 140 139 70 | | 114.60 | |
| 141 139 70 | | 229.70 | |
| 140 140 70 | | 29.60 | |
| 141 140 70 | | 4.38 | |
| Primary photon # 21 | | Total E. Dept: 464.10 | |
| 139 139 79 | | 84.70 | |
| 139 140 79 | | 43.90 | Photoelectric |
| 139 140 80 | | 158.00 | |
| Primary photon # 53 | | Total E. Dept: 286.60 | |
| 152 146 48 | | 194.90 | |
| 153 145 49 | | 22.95 | |
| 152 146 49 | | 11.25 | |
| 154 145 57 | | 32.03 | |
| 139 139 77 | | 53.98 | |
| 140 140 77 | | 203.80 | Compton |
| 139 139 78 | | 86.93 | |
| 139 140 78 | | 14.98 | |
| 140 140 78 | | 41.11 | |
| Primary photon # 42 | | Total E. Dept: 662.00 | |
| 139 139 60 | | 32.92 | |
| 139 139 61 | | 41.90 | |
| 139 140 61 | | 58.60 | |
| 140 140 61 | | 94.60 | |
| 141 140 61 | | 5.38 | |
| 140 141 61 | | 54.10 | Photoelectric |
| 141 141 61 | | 177.00 | |
| 140 140 62 | | 43.50 | |
| 140 141 62 | | 23.15 | |
| 141 141 62 | | 131.00 | |
| Primary photon # 99 | | Total E. Dept: 662.00 | |
| 173 154 9 | | 75.20 | |
| 139 139 19 | | 36.20 | |
| 139 139 20 | | 375.00 | |
| 206 121 42 | | 30.90 | Compton |
| 206 122 42 | | 144.00 | |
| Primary photon # 35 | | Total E. Dept: 662.00 | |

E. Dept.: represents Energy Deposition

It is important to note that electrode foils with various thicknesses were taken into account in this simulation study, and the efficiency parameter for each thickness was measured. Based on the numerical trial assessment, the optimum thickness was obtained at 0.01 cm.

Figure 3 illustrates efficiency variations as the function of photon energies for different semi-conductor detectors obtained in the current study. The photon energy ranges from 28 keV to 1250 keV using standard sources in isotropic fashion. As demonstrated in this

figure, for all detectors, the efficiency factor is reduced by increased energy of source. The maximum efficiency is at 28 keV photons emitted from Ir-192.

As indicated, the maximum efficiency for all energies belongs to CZT with gold foils that are superior, as compared with other detectors. On the contrary, SiLi detector has the minimum efficiency at different energies.

Table 2. Selected results from the interaction of 662 keV photons with Au/CZT/Au detector (Au represents gold foils as electrodes around CZT.)

| Mesh coordinate inside the detector x y z | Energy deposition at each interaction (keV) | Type of interaction |
|--|---|---------------------|
| 139 139 55 | 662.00 | Photoelectric |
| Primary photon # 41 | Total E. Dept: 662.00 | |
| 139 139 76 | 116.60 | Compton |
| 134 138 77 | 69.038 | |
| 137 139 78 | 270.10 | |
| 138 139 78 | 203.40 | |
| 137 140 78 | 2.75 | |
| Primary photon # 21 | Total E. Dept: 662.00 | |
| 148 131 45 | 243.40 | Compton |
| 139 139 51 | 67.058 | |
| 140 138 53 | 153.20 | |
| 140 138 54 | 133.00 | |
| 138 141 54 | 65.30 | |
| Primary photon # 64 | Total E. Dept: 662.00 | |
| 140 137 68 | 67.19 | Compton |
| 140 140 68 | 111.90 | |
| 139 139 72 | 152.30 | |
| 138 139 73 | 120.30 | |
| 139 139 73 | 210.00 | |
| Primary photon # 42 | Total E. Dept: 662.00 | |
| 139 139 24 | 662.00 | photoelectric |
| Primary photon # 53 | Total E. Dept: 662.00 | photoelectric |
| 138 138 33 | 319.70 | |
| 139 138 33 | 9.63 | |
| 138 139 33 | 125.40 | |
| 139 139 33 | 88.48 | |
| 138 138 34 | 18.52 | |
| 138 139 34 | 1.53 | |
| 139 139 34 | 98.80 | |
| Primary photon # 12 | Total E. Dept: 662.00 | Compton |
| 139 139 27 | 389.00 | |
| 119 151 42 | 0.98 | |
| 118 152 43 | 56.80 | |
| 118 153 43 | 214.90 | |
| Primary photon # 79 | Total E. Dept: 662.00 | photoelectric |
| 134 138 21 | 55.71 | |
| 135 138 21 | 11.48 | |
| 139 139 22 | 269.20 | |
| 139 139 23 | 325.65 | |
| Primary photon # 99 | Total E. Dept: 662.00 | |

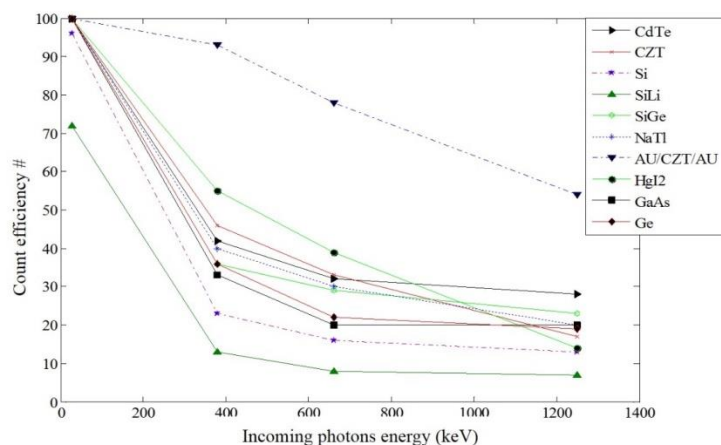


Figure 3. Detector efficiency variations at different energies of photon sources using various common available detectors

Discussion

In the current study, a quantitative investigation was conducted on the behavior of CZT detector against photons at the microdosimetry scale by monitoring all

possible collisions. The results indicated the three-dimensional collision locations of each primary photon in association with deposited energy, accordingly.

Table 3. Comparing the overall results of photon incidents at Cadmium Zinc Telluride detector with and without implementing gold foils

| Type of detector | Type of interactions | | The number of particles counted (from 100 photons) | Total number of occurred interactions |
|------------------|----------------------|---------------|--|---------------------------------------|
| | Compton | Photoelectric | | |
| CZT | 9 | 6 | 39 | 173 |
| Au/CZT/Au | 33 | 37 | 78 | 251 |

CZT: Cadmium Zinc Telluride

Moreover, the total energy deposition was calculated by the addition of energy depositions of all collisions caused by each unique incident photon inside detector sensitive volume.

As displayed in Table 1, the photoelectric effect and Compton scattering phenomenon were recognized according to the location of deposited energies and the amount of energy deposition. In photoelectric phenomena, the energetic emitted electron is responsible for the gross ionizing process on a 3D electron trajectory through detector sensitive volume until finishing electron energy. This process is depicted in Table 1 for primary photon with index #81, as typical example. As illustrated, the total 662 keV photon energy has been transferred to electron; thereafter, it was deposited in a small sub-region, including electron ranging from (139, 139, 39) coordinate to (141, 139, 41) coordinate of meshes. Nonetheless, for some photoelectric effect, photoelectron does not spend all its kinetic energy and may leave detector volume with the rest of its energy (e.g., a primary photon with index #53 in Table 1). This occurs while photoelectric phenomena affect the outer edge in the downstream part of detector volume, as opposed to the beam propagation direction.

In contrast, during Compton scattering, several gross ionizing occurred at different parts of detector volume with remarkable distances (versus electron range) far away from each other. This outcome is indicated in Table 1 for photon with index #35. For this event, the scattered photon may cause ionizing at three parts: part I: starting from 9 to 19, part II: starting from 19 to 20, and part III: starting from 20 to 42 in-depth direction.

In practice, two gold foils are used at both sides of detector as electrode. In the current study, the effect of these foils on the number of interactions and the amount of deposited energy was thoroughly assessed (Table 2). As demonstrated in this table, detector efficiency will be enhanced by depositing remarkable energy of primary photons. Therefore, the use of gold foils as electrodes increases the number of collisions and the occurrence of photoelectric phenomenon more than Compton scattering. Table 3 displays the effects of gold foils on detector efficiency by summarizing total collisions.

Moreover, high energy electrons ejected from upstream gold foil with a high atomic number into the detector body may increase incidents. In other hand, the number of photoelectric phenomena is more than Compton Scatterings taking into account golden electrodes. Therefore, the probability of photoelectric effect is higher and detector efficiency will be improved by implementing gold foils during the simulation

process. Detector efficiency with and without electrodes was 78% and 39%, respectively, and the number of interactions increased from 173 to 251.

Conclusion

In the current study, a microdosimetry simulation was performed on CZT compound semi-conductor detector by monitoring all possible collisions against photons as an incident beam. To this end, the FLUKA code was used, and the detector efficiency parameter was taken into account for the final analysis. As evidenced by the obtained results, the collisions location of each incident photon, as well as the deposited energy at each location, were achieved. It enables us to quantitatively investigate the photoelectric effect and Compton scattering inside detector sensitive volume.

In addition, two gold foils were located on both sides of the detector as electrode, and the effect of these foils on the quantity and type of interactions were taken into account. The obtained results can be of great help in understanding the process which is taking place while photons interact with detector sensitive volume from a microdosimetry point of view. In this way, detector dimension, material, as well as electrodes type and thickness can be considered to analyze the number of total collisions and detector efficiency.

References

1. Fritz SG, Shikhaliev PM. CZT detectors used in different irradiation geometries simulations and experimental results. *Med phy.* 2009; 36: 1098-108.
2. Verger L, Gentet M C, Geraud L, Guillemaud R, Mestais C, Monnet O, et al. Performance and perspectives of a CdZnTe-based gamma camera for medical imaging. *Nucl Sci, IEEE Transactions.* 2004; 51: 3111-7.
3. Lee YJ, Ryu HJ, Cho HM, Lee SW, Choi YN, Kim HJ. Optimization of an ultra-high-resolution parallel-hole collimator for CdTe semiconductor SPECT system. *Journal of Instrumentation.* 2013;8(01):C01044.
4. Shor A, Eisen Y, Mardor I. Optimum spectroscopic performance from CZT Gamma and X-ray detectors with pad and strip segmentation. *Nucl. Instrum. Methods. Phys. Res A.* 1999; 428 :182-92.
5. Knoll GF. *Radiation detection and measurement.* John Wiley & Sons; 2010 Aug 16.
6. Nakhostin M, Esmaili Torshabi A. The influence of electron track lengths on the γ -ray response of compound semiconductor detectors. *Nucl Instrum Methods Phys Res A.* 2015; 797: 255-9.
7. Park SH, Ha JH, Lee JH, Cho YH, Kim HS, Kang SM, et al. Fabrication of CZT Planar-Type Detectors

- and Comparison of their Performance. *J Nucl Sci Tech.* 2008; 45: 348-51.
8. Bradley PD, Rosenfeld AB, Zaider M. Solid state microdosimetry. *Nucl Instrum Methods Phys Res B.* 2001; 184: 135-57.
 9. Abbaspour S, Mahmoudian B, Pirayesh Islamian J. Cadmium Telluride Semiconductor Detector for Improved Spatial and Energy Resolution Radioisotopic Imaging. *World J Nucl Med.* 2017; 16: 101-7.
 10. Kellerer AM. An assessment of wall effects in microdosimetric measurements. *Radiat Res.* 1971; 47: 377-86.
 11. Bradley PD, Rosenfeld AB, Lee KK, Jamieson DN, Heiser G, Satoh S. Charge collection and radiation hardness of a SOI microdosimeter for medical and space applications. *IEEE transactions on nuclear science.* 1998 Dec;45(6):2700-10.
 12. Cornelius I, Siegele R, Rosenfeld AB, Cohen DD. Ion beam induced charge characterisation of a silicon microdosimeter using a heavy ion microprobe. *Nuclear Instruments and Methods in Physics Research Section B: Beam Interactions with Materials and Atoms.* 2002;190(1-4):335-8.
 13. Shah KS, Lund JC, Olschner F. Charge collection efficiency in a semiconductor radiation detector with a non-constant electric field. *IEEE Trans Nucl Sci.* 1990; 37:183-6.
 14. Zikovsky L, Chah B. A computer program for calculating Ge (Li) detector counting efficiencies with large volume samples. *Nuclear Instruments and Methods in Physics Research Section A: Accelerators, Spectrometers, Detectors and Associated Equipment.* 1988;263(2-3):483-6.
 15. Selim YS, Abbas MI, Fawzy MA. Analytical calculation of the efficiencies of gamma scintillators. Part I: Total efficiency for coaxial disk sources. *Radiation Physics and Chemistry.* 1998;53(6):589-92.
 16. Jehouani A, Ichaoui R, Boulkheir M. Study of the NaI(Tl) efficiency by Monte Carlo method. *Appl Radiat Isotopes.* 2000; 53: 887-91.
 17. Abbas MI. Analytical formulae for well-type NaI (Tl) and HPGe detectors efficiency computation. *Applied Radiation and Isotopes.* 2001;55(2):245-52.
 18. Fasso A, Ferrari A, Ranft J, Sala PR. FLUKA: a multi-particle transport code. *CERN-2005-10;* 2005.
 19. Böhlen TT, Cerutti F, Chin MP, Fassò A, Ferrari A, Ortega PG, et al. The FLUKA code: developments and challenges for high energy and medical applications. *Nuclear data sheets.* 2014 Jun 1;120:211-4.
 20. Battistoni G, Bauer J, Boehlen TT, Cerutti F, Chin MP, Dos Santos Augusto R, Ferrari A, Ortega PG, Kozłowska W, Magro G, Mairani A. The FLUKA code: an accurate simulation tool for particle therapy. *Frontiers in oncology.* 2016;6:116.
 21. Guthoff M, de Boer W, Müller S. Simulation of beam induced lattice defects of diamond detectors using FLUKA. *Nucl. Instrum. Methods Phys. Res A.* 2014; 735: 223-8.
 22. Yalcin S, Gurler O, Kaynak G, Gundogdu O. Calculation of total counting efficiency of a NaI(Tl) detector by hybrid Monte-Carlo method for point and disk sources. *Appl Radiat Isotopes.* 2007; 65: 1179-86.
 23. Andersen V, Ballarini F, Battistoni G, Campanella M, Carboni M, Cerutti F, et al. The FLUKA code for space applications: recent developments. *Adv Space Res.* 2004; 34:1302-10.
 24. Mairani A, Brons S, Cerutti F, Fasso A, Ferrari A, Kramer M, et al. The FLUKA Monte Carlo code coupled with the local effect model for biological calculations in carbon ion therapy. *Phys Med Biol.* 2010; 55:4273-89.
 25. Vetter K. Recent Developments in the Fabrication and Operation of Germanium Detectors. *ANNU REV NUCL PART S Annu Rev Nucl Part S.* 2007; 57: 363-404.
 26. Luke PN and Amman M. Room-Temperature Replacement for Ge Detectors -Are We There Yet?. *IEEE Trans Nucl Sci.* 2007; 54: 834-42.
 27. Johnson LC, Campbell DL, Hull EL, Peterson TE. Characterization of a high-purity germanium detector for small-animal SPECT. *Physics in Medicine & Biology.* 2011;56(18):5877.
 28. Walton JT, Pehl RH, Wong YK, Cork CP. Si (Li) X-ray detectors with amorphous silicon passivation. *IEEE Transactions on Nuclear Science.* 1984;31(1):331-5.
 29. Owens A, Peacock A. Compound semiconductor radiation detectors. *Nuclear Instruments and Methods in Physics Research Section A: Accelerators, Spectrometers, Detectors and Associated Equipment.* 2004;531(1-2):18-37.